Journal of Alloys and Compounds 501 (2010) 371–374

Contents lists available at ScienceDirect

Journal of Alloys and Compounds

journal homepage: www.elsevier.com/locate/jallcom

Elaboration and characterization of transparent $GdTaO_4:Tb^{3+}$ thick films fabricated by sol–gel process

Mu Gu*, Liping Zhu, Xiaolin Liu, Shiming Huang, Bo Liu, Chen Ni

Shanghai Key Laboratory of Special Artificial Microstructure Materials & Technology, Department of Physics, Tongji University, Shanghai 200092, PR China

ARTICLE INFO

Article history:
Received 23 February 2010
Received in revised form 3 April 2010
Accepted 7 April 2010
Available online 24 April 2010

Keywords:
Thick films
Sol–gel processes
Optical properties
Luminescence

ABSTRACT

Transparent $GdTaO_4:Tb^{3+}$ polycrystalline thick films have been successfully synthesized using sol–gel technique. The critical thickness of the film was 760 nm and the surface was crack-free and smooth. The thick film particle size was 25 nm and the powder particle size was over micron. In comparison with the thick film phosphors, the charge transfer transition of TaO_4 group and the excitation peak of Tb^{3+} center shifted from 223 to 215 nm and 245 to 255 nm for powder sample, respectively. The higher energy level of the charge transfer indicated the decrease of the covalency of the Ta–O bond in the powder phosphor. The red shift of the 4f-5d excitation band might be attributed to the quantum confinement of Tb^{3+} in the film phosphor. The decay times of $GdTaO_4:Tb^{3+}$ thick film and powder phosphors were 0.79 and 1.02 ms, respectively.

1. Introduction

Gadolinium tantalate was proved to be an efficient host for X-ray luminescence material due to its advantages of high density, stable chemical properties, strong irradiation hardness, and good X-ray absorption. Many researchers have investigated the luminescent properties of Eu^{3+}, Tb^{3+} doped tantalate powders and films [1–10]. It indicated that the $GdTaO_4:Tb^{3+}$ is one of the potential green emission phosphors.

Compared with powder, thin film is more outstanding because of high contrast and resolution, superior thermal conductivity, as well as high degree of uniformity and better adhesion. Sol–gel coating technique is widely used in the fabrication of functional films. However, the critical thickness, i.e., the maximum thickness achievable without crack formation via non-repetitive deposition, is often less than 0.1 μm for non-silicate crystalline films [11]. Recently, Kozuka et al. reported that the incorporation of a high boiling point reagent such as polyvinylpyrrolidone (PVP) into precursor solutions is an effective way to improve the critical thickness over submicron or micron and form the crack-free and optical transparent thick films [11–14]. More recently, we successfully prepared $GdTaO_4:Eu^{3+}$ and $Gd_2O_3:Eu^{3+}$ thick films with the assistance of PVP [15,16].

Compared with Eu^{3+}, the energy transfer from host lattice to Tb^{3+} ions in $GdTaO_4$ occurs not only from the TaO_4 group to Tb^{3+} on nearest neighbor Gd-sites, but also to Tb^{3+} on next-nearest and even on next to next-nearest neighbor Gd^{3+}-sites [2]. Therefore, it is expected to get higher luminescence efficiency for $GdTaO_4$ doping with Tb. Additionally, Tb_4O_7 is more difficult to be dissolved than Eu_2O_3 in nitric acid. So far, there are no reports on the preparation $GdTaO_4:Tb^{3+}$ thick films and the corresponding characteristics.

In this work, transparent $GdTaO_4:Tb^{3+}$ thick films were synthesized by using the inorganic salt and 2-methoxyethanol solution containing PVP. The morphology, crystallinity and luminescent properties of the thick films were discussed.

2. Experimental

Starting materials were $TaCl_5$ (99.99), Gd_2O_3 (99.95%), Tb_4O_7 (99.99%). Firstly, $TaCl_5$ was dissolved into the mixed solution with 2-methoxythanol (A.R.) and concentrated hydrochloric acid. Stoichiometric amount of Gd_2O_3 and Ta_4O_7 were dissolved in a hot solution of 2-methoxyethanol and certain amount of dilute nitric acid (A.R.). The prepared solutions were mixed together and the mixture was stirred for about ten minutes. Then PVP (an average molecular weight of 1.3×106) dissolved in 2-methoxyethanol and ion-exchanged water were added into the mixture by stirring and get the sol. For the sake of the determination of the optimal Tb doping concentration, $Gd_{1-x}Tb_xTaO_4$ ($x = 0.02, 0.04, 0.06, 0.08, 0.10, 0.12, 0.14, 0.16, 0.18$) powder samples were prepared with the same process. The result indicated the optimal Tb doping content was at $x = 0.12$. For fabrication of the thick films, the molar composition of the coating sol was selected as $Ta:Gd:Tb:PVP:H_2O = 1:0.88:0.12:0.12:3.73$. The deposited gel films after spin-coated on a silica glass substrates were sintered at 400 °C for 90 min and up to 1200 °C at the heating rate of 4 °C/min, then they were finally annealed at 1200 °C for 200 min to obtain dense and crystalline thick films. In order to compare with film samples, powder samples were also prepared by the rest sol with the same heating procedure. The powders are brownish. Zych et al. reported that the brownish was attributed to incorporation of some of the activators Tb^{4+} [17].

The surface morphology and thickness of the thick film were characterized using a Philips XL-30 SEM. The transmittance was examined by a JASCO V-570 ultraviolet–visible–near infrared spectrophotometer. The structure of the samples

* Corresponding author. Tel.: +86 021 65980219; fax: +86 021 65980219.
E-mail address: mgu@tongji.edu.cn (M. Gu).

0925-8388/$ – see front matter © 2010 Elsevier B.V. All rights reserved.
doi:10.1016/j.jallcom.2010.04.109

was analyzed by a Rigaku D/max-2550 X-ray diffractometer with Cu Kα radiation (λ = 0.154056 nm) operated at 40 kV and 100 mA. Particle size distribution of the powder was carried out on granulometer LB 550. The luminescent spectra and the decay curves were measured on a Perkin-Elmer LS-55 spectrofluorometer.

3. Results and discussion

Crack-free $GdTaO_4$:Tb^{3+} thick film has been prepared from solutions containing PVP via single-step deposition. The thick film is fairly transparent (Fig. 1(a)), smooth and relatively dense (Fig. 1(b)). The film thickness also characterized by SEM is about 760 nm as illustrated in Fig. 1(c). The incorporation of PVP leads to a increase in the thickness of films, because the C=O groups of the PVP can hybridize with the OH groups in the surface of the gel particles through strong hydrogen bonds, which can suppress the reaction of the condensation and hydrolysis in the sol and promote the structural relaxation in the films [11,18].

The optical transparency directly affects the light yield of the luminescence films. Fig. 2 shows the transmission spectrum of the $GdTaO_4$:Tb^{3+} thick film. Quickly dropping signal around 210 nm is observed, indicating very strong absorption of the material in this spectral region. A high transmittance is achieved in the visible region. Additionally, the absorption coefficient could be calculated through $\alpha = -\ln\ T/d$, where T and d denote the transmittance and the film thickness, respectively. According to the relation of $\alpha \propto (h\nu - E_{opt})^{1/2}$, where $h\nu$ and E_{opt} indicate the photon energy and the optical band gap, respectively, we can obtain E_{opt} by plotting $(\ln T)^2$ as a function of $h\nu$ and drawing a tangential line near the absorption edge. The result is given in the inset of Fig. 2. The absorption edge of the thick film is about 5.7 eV, which is larger than that of the thin film (5.3 eV) [10]. This could be attributed to the difference in the processing conditions, leading to the different way in the growth of grains.

$GdTaO_4$ usually exhibits two structure types at room temperature [3,19], i.e., M-type (fergusonite) and M′-type, and it can convert to T-type structure (scheelite) at the temperature higher than 1400 °C. In addition, $GdTaO_4$ has another high temperature structure: O-type ($Gd_{0.33}TaO_3$). The most significant difference between M- and M′-type is in the coordination of the Ta atoms. For M-type structure, the Ta atoms are in a distorted cube, while the Ta atoms are in distorted octahedron coordination with six Ta–O bonds for the M′-type. Although M- and M′-type are both efficient luminescent host materials, M′-type $GdTaO_4$ has superior luminescent efficiency, which is nearly two times greater for pure M′-type $GdTaO_4$ than M-type $GdTaO_4$ due to the difference between the M and M′ structures [3]. Fig. 3 shows the X-ray diffraction patterns of the $GdTaO_4$:Tb^{3+} powder and thick film samples. It reveals that both of $GdTaO_4$:Tb^{3+} powder and thick film belong to M′-type (PDF72-2017) except for the extra diffraction peak in powder sample, which belongs to T-type (PDF 39-0728) and O (0 0 4) (PDF18-0526). That is to say the crystallization of the thick film is more pure than that of powder sample. Additionally, the grain size D was calculated by Scherrer formula $D = K\lambda/\beta\cos\theta$, where λ is the wavelength of the X-ray (0.154056 nm), β is the FWHW (full width at half maximum) of the (1 1 1) main peak, θ is the Bragg diffraction angle, and parameter K equals to 0.89. The average grain sizes of the film and powder samples are about 25 and 39 nm, respectively. The average particle size of the thick film, which can be estimated from the calculated results by Scherrer formula [10], is 25 nm, while the particle size of the powder was over micron as shown in Fig. 4.

The emission and excitation spectra of the $GdTaO_4$:Tb^{3+} thick film and powder are presented in Fig. 5. The emission peaks are at around 490, 546, 588 and 620 nm, which can be ascribed to the transitions of the $^5D_4 \rightarrow {}^7F_J$ (J = 6, 5, 4, 3) as shown in Fig. 5(a). In the range of 350–450 nm, no peaks can be seen, which indicated that emission originated from the transitions

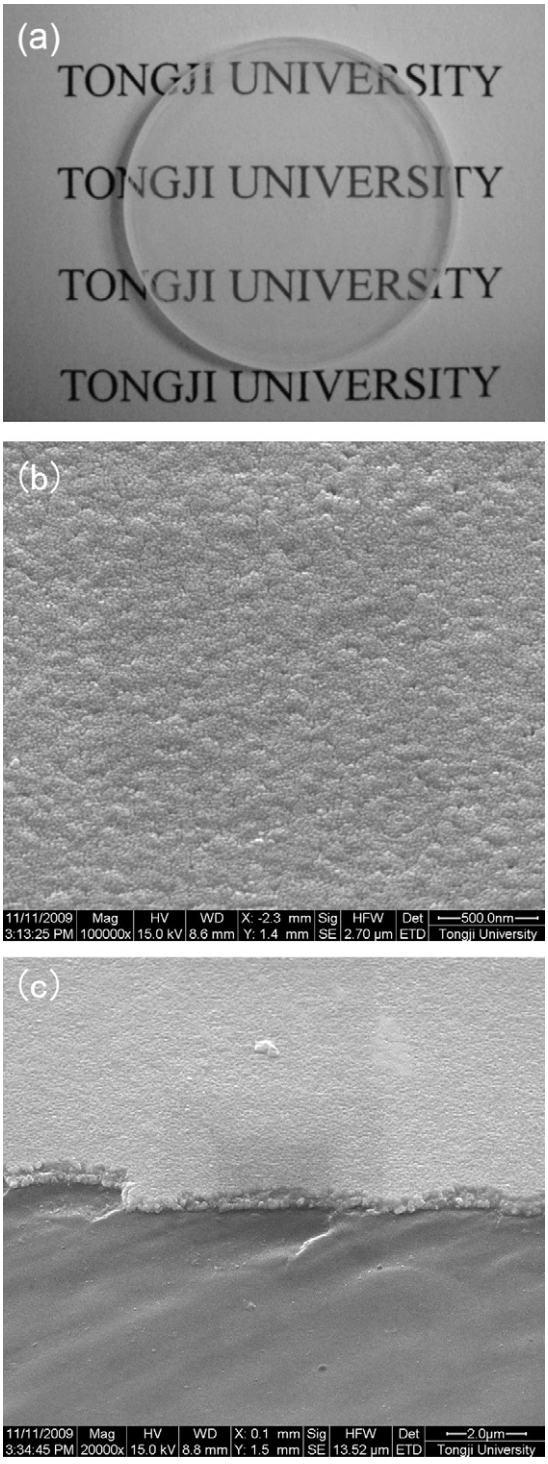

Fig. 1. Photographs of the $GdTaO_4$:Tb^{3+} thick film by single-step spin coating after fired at 1200 °C for 200 min, (a) the whole coating sample, (b) surface morphology, (c) SEM photograph of $GdTaO_4$:Tb^{3+} thick film.

of $^5D_3$ to ^7F_J quenched here by cross-relaxation in the form of $Tb(^5D_3) + Tb(^7F_6) \rightarrow Tb(^5D_4) + Tb(^7F_6)$ because of high Tb^{3+} concentration.

In Fig. 5(b), a dominant broad band near 223 nm in excitation spectra, monitoring 546 nm emission, originated from the excitation of TaO_4 charge transfer state (CTS) in which an electron is transferred from the fully occupied valence band formed by O^{2-} 2p to the empty conduction band of Ta^{5+} 5d [20]. The other peaking around 245 nm belongs to the transition of Tb^{3+} from $4f^8$ to

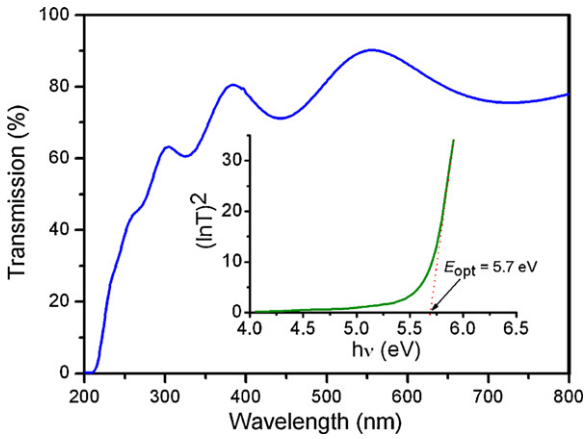

Fig. 2. Transmission spectrum of the $GdTaO_4$:Tb thick film.

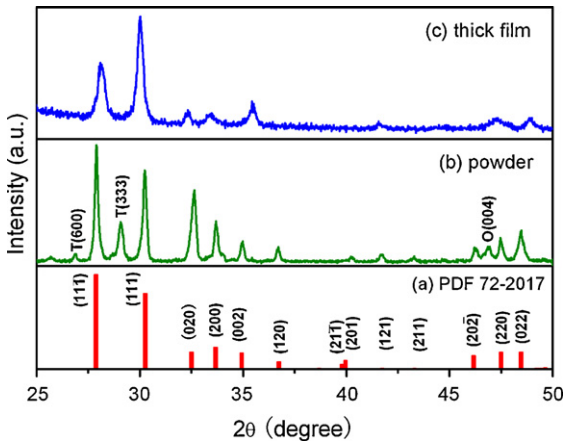

Fig. 3. X-ray diffraction patterns for (a) $GdTaO_4$:Tb^{3+} standard PDF, (b) powder and (c) thick film samples.

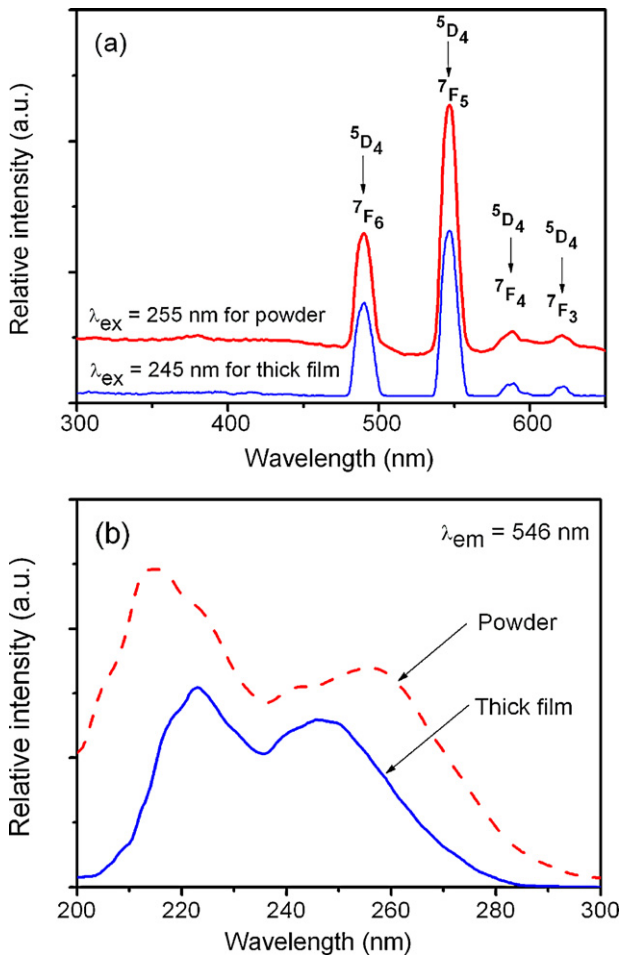

Fig. 5. (a) Emission and (b) excitation spectra of the $GdTaO_4$:Tb^{3+} film and powder samples.

higher $4f^75d^1$ levels [1]. From Fig. 5(b), it clearly indicates that the excitation energy can be transferred from TaO_4 groups to Tb^{3+} ions efficiently. That is to say, high luminescence efficiency would be achieved under ionizing radiation excitation.

In comparison with the film sample, the CTS of TaO_4 and 4f-5d transition of Tb^{3+} for powder sample are shifted from 223 to 215 nm and 245 to 255 nm, respectively. The blue shift of the CTS transition implies the decrease of the covalency of the Ta–O bond [9] in the powder because of the smaller radius and larger electronegativity Tb^{4+} than Tb^{3+} existence. Then it will attract the electrons of O^{2-} more strongly, so that the electron cloud density of the O^{2-} ion decreases and it needs more energy for the electron transfer from O^{2-} to Ta^{5+}. The red shift of the 4f-5d transition might be attributed to quantum confinement of Tb^{3+} in the thick film, because the particle size of powder was over micron and then the peak of the Tb 4f-5d transition moves to lower energy [21].

Decay time is also an important parameter of luminescence materials. The decay curves of $^5D_4 \rightarrow {}^7F_5$ transition for the $GdTaO_4$:Tb^{3+} film and powder samples are shown in Fig. 6. The decay curves for $^5D_4 \rightarrow {}^7F_5$(546 nm) of Tb^{3+} ions also be fitted by

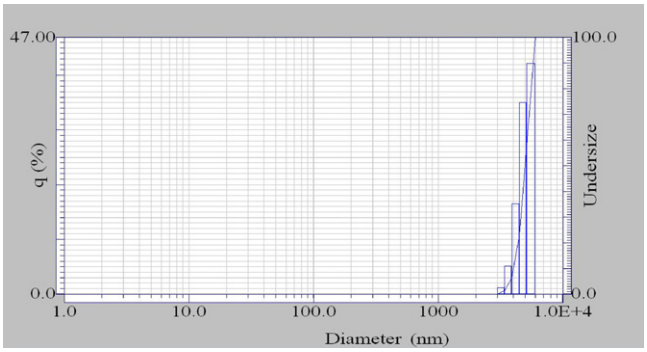

Fig. 4. Particle size distribution of $GdTaO_4$:Tb powders.

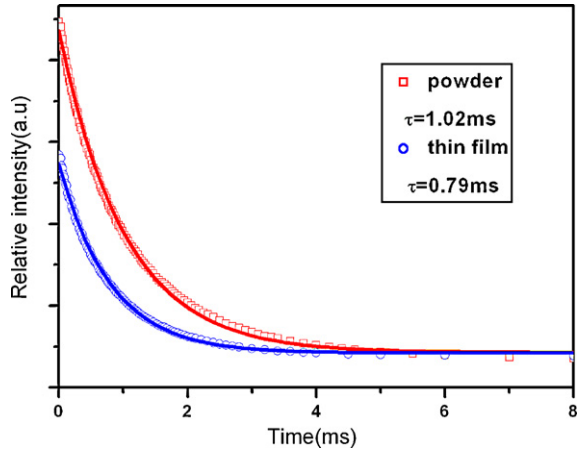

Fig. 6. Decay curves of $^5D_4 \rightarrow {}^7F_5$ transition for $GdTaO_4$:Tb^{3+} film and powder samples under 245 and 255 nm UV excitation, respectively.

single exponential function. The decay times of the thick film and the powder are 0.79 and 1.02 ms, respectively. The shorter lifetime for the film sample may be due to the non-radiative centers or defects.

4. Conclusion

Homogenous, crack-free, dense transparent thick $GdTaO_4:Tb^{3+}$ films were deposited on silica glass substrates from the inorganic salt and 2-methoxyethanol solution containing PVP via sol–gel technique. The thickness was achieved 0.76 μm. The XRD results show that crystallization of the thick film is more pure than that of powder sample. The particle size of the thick film is 25 nm and the particle size of the powder was over micron. In comparison with the thick film phosphor, the charge transfer transition of TaO_4 group and the excitation peak of Tb^{3+} center shifted from 223 to 215 nm and 245 to 255 nm for powder sample, respectively. The higher energy level of the charge transfer indicated the decrease of the covalency of the Ta–O bond in the powder phosphors. The red shift of the 4f-5d excitation band could be attributed to the quantum confinement of Tb^{3+} in the film sample. The decay times of $GdTaO_4:Tb^{3+}$ thick films are 0.79 ms.

Acknowledgments

This work is supported by National Natural Science Foundation of China (Grant Nos. 50672068, 10974143 and 10875085), and Committee of Science and Technology Shanghai Municipality (Contract No.07DZ22302).

References

[1] M.J.J. Lammers, G. Blasse, Mater. Res. Bull. 19 (1984) 759–768.
[2] G. Blasse, A. Bril, J. Lumin. 3 (1970) 109–131.
[3] L.H. Brixner, H.Y. Chen, J. Electrochem. Soc.: Solid-State Sci. Technol. 130 (1983) 2435–2443.
[4] B. Li, Z.N. Gu, Y. Dong, J.H. Lin, M.Z. Su, Chem. Res. Chin. Univ. 15 (1999) 226–231.
[5] B. Li, Z.N. Gu, J.H. Lin, M.Z. Su, Mater. Res. Bull. 35 (2000) 1921–1931.
[6] B. Li, Z.N. Gu, J.H. Lin, M.Z. Su, J. Mater. Sci. 35 (2000) 1139–1143.
[7] M. Nazarov, B. Tsukerblat, C.C. Byeon, I. Arellano, E.J. Popovici, D.Y. Noh, Appl. Opt. 48 (2009) 17–21.
[8] B. Liu, M. Gu, X.L. Liu, K. Han, S.M. Huang, C. Ni, G.B. Zhang, Z.M. Qi, Appl. Phys. Lett. 94 (2009) 061906.
[9] X.L. Liu, K. Han, M. Gu, L.H. Xiao, C. Ni, S.M. Huang, B. Liu, Solid State Commun. 142 (2007) 680–684.
[10] M. Gu, X. Xu, X.L. Liu, L.Q. Qiu, R. Zhang, J. Sol–Gel Sci. Technol. 35 (2005) 193–196.
[11] H. Kozuka, M. Kajimura, J. Am. Ceram. Soc. 83 (2000) 1056–1062.
[12] G.T. Park, J.J. Choi, C.S. Park, J.W. Lee, H.E. Kim, Appl. Phys. Lett. 85 (2004) 2322–2324.
[13] H. Kozuka, A. Higuchi, J. Am. Ceram. Soc. 86 (2003) 33–38.
[14] H. Kozuka, S. Takenaka, H. Tokita, M. Okubayashi, J. Euro. Ceram. Soc. 24 (2004) 1585–1588.
[15] X.L. Liu, K. Han, M. Gu, S.M. Huang, B. Liu, C. Ni, Appl. Surf. Sci. 255 (2009) 4680–4683.
[16] X.L. Liu, F. Zhou, M. Gu, S.M. Huang, B. Liu, C. Ni, Opt. Mater. 31 (2008) 126–130.
[17] E. Zych, P.J. Dereń, W. Strçk, A. Meijerink, W. Mielcarek, K. Domagala, J. Alloys Compd. 323–324 (2001) 8–12.
[18] H. Kozuka, M. Kajimura, T. Hirano, K. Katayama, J. Sol–Gel Sci. Technol. 19 (2000) 205–209.
[19] G.M. Wolten, Acta. Cryst. 23 (1967) 939–944.
[20] J.T. Waber, D.T. Cromer, J. Chem. Phys. 42 (1965) 116.
[21] R.S. Yadav, A.C. Pandey, J. Alloys Compd. 494 (2010) L15.